JOC Article

N_i-to-N_{i+3}-Ethylene-Bridged Partially Modified Retro-Inverso Tetrapeptide β-Turn Mimetic: Design, Synthesis, and Structural Characterization†

Yinglin Han,‡ Craig Giragossian,§ Dale F. Mierke,§,|| and Michael Chorev*,‡

Department of Medicine, Bone and Mineral Metabolism Unit, Charles A. Dana and Thorndike Laboratories, Beth Israel Deaconess Medical Center—Harvard Medical School, Boston, Massachusetts 02215, Department of Chemistry and Department of Molecular Pharmacology, Division of Biology and Medicine, Brown University, Providence, Rhode Island 02912

chorev@hms.harvard.edu

Received October 29, 2001

A 10-membered heterocyclic ring system 1,3,8-trisubstituted 2,5,7-trioxo-1,4,8-triazadecane that represents a N_i-to-N_{i+3}-ethylene-bridged partially modified retro-inverso tetrapeptide β-turn mimetic (EBRIT-BTM) has been designed, synthesized, and structurally analyzed. These compounds utilize an ethylene bridge to replace the $CO_i\cdots HN_{i+3}$ 10-membered hydrogen bond of standard β-turns. The *N*,*N*′-ethylene-bridged dimer was obtained in 90% yield by reductive alkylation of phenylalanylamide with a *tert*-butyl *N*-(9-fluorenylmethyloxycarbonyl),*N*-(2-formylmethyl)-glycinate. An orthogonal protection strategy and HATU-mediated couplings allowed efficient stepwise additions of monomeric building blocks leading to a N_i-to-N_{i+3}-ethylene-bridged linear precursor: H-Asp-(OcHex)-*N*Gly-OBu^t HO_2CCH_2CO-*N*Phe-NH_2. Further elaboration of the linear precursor generated the ethylene-bridged model compounds H_2N-*r*Phe*N*-*m*Gly-Asp-*N*Gly-OH (**16**) and Ac-*g*Phe*N*-*m*Gly-Asp-*N*Gly-OH (**18**) (*g*, *gem*-diaminoalkyl; *m*, malonyl; and *r*, direction-reversed amino acid residue) in 44 and 39% yields, respectively. The structural features of the two EBRIT-BTM compounds were determined using ^{1}H NMR and extensive computer simulations. The results indicate that the 10-membered rings are conformationally constrained with well-defined structural features and that the three amide bonds in the ring are in the trans orientation. The topological arrangement of the residues in the ring system closely resembles a type II′ β-turn. Transformation of $CONH_2$ in the N-terminal amino acid residue of **16** into $NHCOCH_3$ in **18** resulted in the formation of a hydrogen bond between the NH of *g*Phe-$COCH_3$ and the C-terminal carboxyl of Gly, initiating an antiparallel β-sheet. The formulation of the concept applying a minimalistic structural elaboration approach and the synthetic exploration, together with the conformational analysis, offer a new molecular scaffolding system and a true tetrapeptide secondary structure mimetic that can be used to generate peptidomimetics of biological interest.

Introduction

Reverse turns, such as β-turns, are documented to be important structural elements in bioactive conformations of many peptides. Peptide hormones such as angiotensin II,[1] gonadotrophin releasing hormone (GnRH),[2,3] and somatostatin,[4,5] as well as other bioactive peptides such as Arg-Gly-Asp-based integrin antagonists,[6,7] fibrinopeptide A,[8] prohormones,[9,10] and a CD4-derived motif that

* To whom correspondence should be addressed. Phone: (617) 667-0901. Fax: (617) 667-4432.

† Prefixes *g* and *m* preceding the standard three-letter notation for amino acid residues indicate the *gem*-diaminoalkyl and 2-alkyl-substituted malonyl residues corresponding to the side chain characterizing the amino acid specified by the three-letter notation. The prefix *r* preceding the standard three-letter notation for amino acid residues indicates the incorporation of this amino acid in the reversed-sense orientation, namely, NH←CO

‡ Beth Israel Deaconess Medical Center—Harvard Medical School.

§ Department of Chemistry, Brown University.

|| Department of Molecular Pharmacology, Division of Biology and Medicine, Brown University.

(1) Plucinska, K.; Kataoka, T.; Yodo, M.; Cody, W. L.; He, J. X.; Humblet, C.; Lu, G. H.; Lunney, E.; Major, T. C.; Panek, R. L.; Schelkun, P.; Skeean, R.; Marshall, G. R. *J. Med. Chem.* **1993**, *36*, 1902−1913.

(2) Nikiforovich, G.; Marshall, G. R. *Int. J. Pept. Protein Res.* **1993**, *42*, 171−180.

(3) Nikiforovich, G. V.; Marshall, G. R. *Int. J. Pept. Protein Res.* **1993**, *42*, 181−193.

(4) Nutt, R. F.; Veber, D. F.; Saperstein, R. *J. Am. Chem. Soc.* **1980**, *102*, 6539−6545.

(5) Brady, S. F.; Paleveda, W. J., Jr.; Arison, B. H.; Saperstein, R.; Brady, E. J.; Raynor, K.; Reisne, T.; Veber, D. F.; Freidinger, R. M. *Tetrahedron* **1993**, 3449−3466.

(6) Bach, A. C., II; Espina, J. R.; Jackson, S. A.; Stouten, P. F. W.; Duke, J. L.; Mousa, S. A.; DeGrado, W. F. *J. Am. Chem. Soc.* **1996**, *118*, 293−294.

(7) Haubner, R.; Schmitt, W.; Holzemann, G.; Goodman, S. L.; Jonczyk, A.; Kessler, H. *J. Am. Chem. Soc.* **1996**, *118*, 7881−7891.

(8) Nakanishi, H.; Chrusciel, R. A.; Shen, R.; Bertenshaw, S.; Johnson, M. E.; Rydel, T. J.; Tulinsky, A.; Kahn, M. *Proc. Natl. Acad. Sci. U.S.A.* **1992**, *89*, 1705−1709.

(9) Rholam, M.; Nicolas, P.; Cohen, P. *FEBS Lett.* **1986**, *207*, 1−6.

10.1021/jo011041w CCC: $22.00
Published on Web 06/19/2002

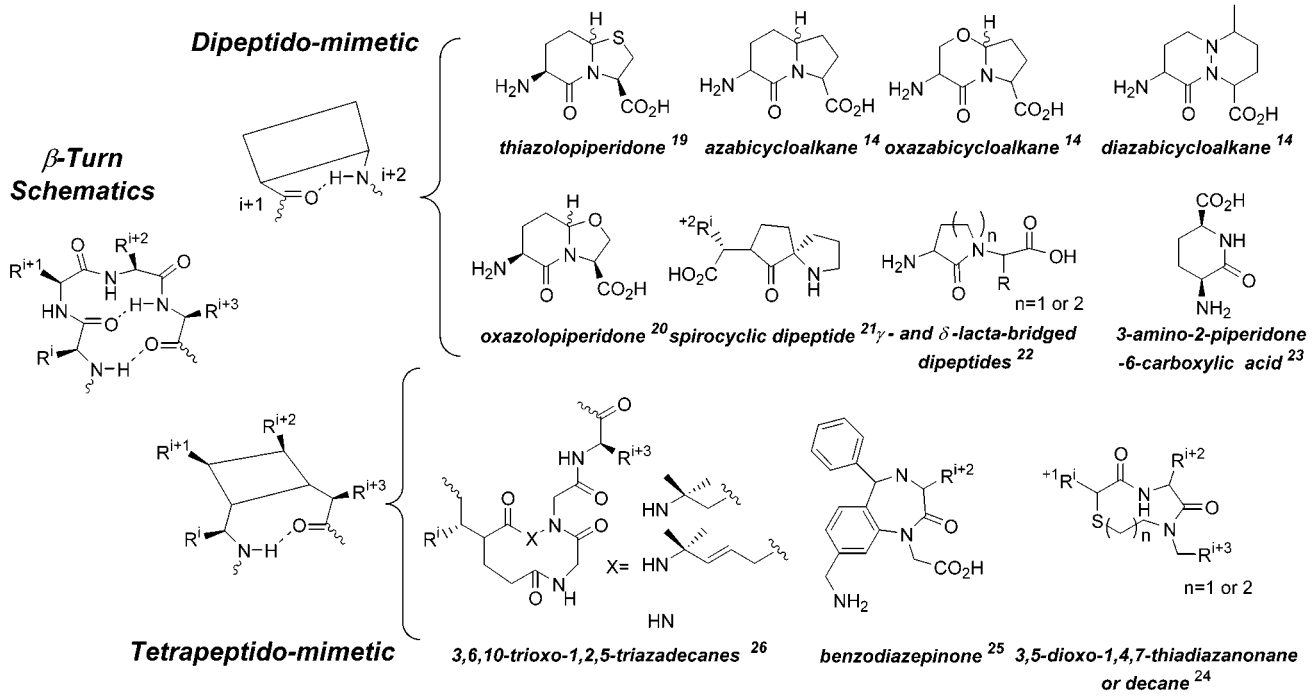

FIGURE 1. Schematics of a β-turn and its dipeptido- and tetrapeptidomimetics are accompanied by selected examples of both modes of mimetics.

binds to gp120,[11] are only a representative sample of β-turn-containing peptides. In these peptides, the β-turns act as a molecular scaffold, presenting recognition motifs and acceptor interaction sites.[12,13]

A β-turn consists of four amino acid residues i-to-$i + 3$ leading to a reversal in the backbone direction, with amino acid residues $i + 1$ and $i + 2$ found in the two corners of the turn. A C═O···HN hydrogen bond between the i and the $i + 3$ residues, respectively, stabilizes almost all of these turns forming a 10-membered intramolecular hydrogen-bonded ring. Different β-turns are distinguished on the basis of the ϕ and ψ torsion angles of the $i + 1$ and $i + 2$ amino acid residues[12,14] or the topology of the side chains involved.[15]

To elucidate the contribution of β-turns to the bioactive conformation of a minimal bioactive sequence, which otherwise is highly flexible, and to enhance and select for a specific profile of pharmacological activity, rigidified β-turn mimetics are developed.[14,16−18] These β-turn-mimicking scaffolds are designed to have a higher avidity for the acceptor by overcoming what otherwise is the inherent entropic cost paid for β-turn formation upon binding to the acceptor. At the same time, in some cases, scaffolding via a fused bicyclic system may cause over-rigidification leading to compromised ligand−acceptor interactions. Nevertheless, these peptidomimetics are potential conformational probes, thus enabling biological activity to be more effectively correlated with structure, and prospective therapeutics overcoming drawbacks such as proteolytic susceptibility and poor bioavailability, typical to many important bioactive peptides.

Many of the β-turn mimetics are mono- and bicyclic systems designed to be dipeptide mimetic replacements of the $i + 1$ and $i + 2$ residues (Figure 1).[14,19−23] In these, attempts are made to correctly position the amino- and carboxyl-termini of the dipeptidomimetic unit to force a reversal of the backbone. However, in general, side chains R_{i+1} and R_{i+2} are not maintained. Several efforts have been directed toward the design of large heterocyclic systems as tetrapeptide mimetics that carry some of the four side chains presented by the original β-turn.[24−26] The restricted conformational space of cyclic peptides and peptidomimetics can be characterized through the use of NMR and computational techniques such as distance geometry, energy minimization, and molecular dynamics.[24,27−30]

(10) Bek, E.; Berry, R. *Biochemistry* **1990**, *29*, 178−183.
(11) Chen, S.; Chrusciel, R. A.; Nakanishi, H.; Raktabutr, A.; Johnson, M. E.; Sato, A.; Weiner, D.; Hoxie, J.; Saragovi, H. U.; Greene, M. I.; Kahn, M. *Proc. Natl. Acad. Sci. U.S.A.* **1992**, *89*, 5872−5876.
(12) Rose, G. D.; Gierasch, L. M.; Smith, J. A. *Adv. Protein Chem.* **1985**, *37*, 1−109.
(13) Muller, G. *Angew. Chem., Int. Ed. Engl.* **1996**, *35*, 2767−2769.
(14) Hanessian, S.; McNaughton-Smith, G.; Lombart, H.-G.; Lubell, W. D. *Tetrahedron* **1999**, *426*, 12789−12852.
(15) Ball, J. B. *Tetrahedron* **1993**, 3467−3478.
(16) Holzemann, G. *Kontakte (Darmstadt)* **1991**, *1*, 3−12.
(17) Ball, J. B.; Alewood, P. *J. Mol. Recog.* **1990**, *3*, 55−64.
(18) Holzemann, G. *Kontakte (Darmstadt)* **1991**, *2*, 55.
(19) Nagai, U.; Sato, K. *Tetrahedron Lett.* **1985**, *26*, 647−650.
(20) Estiarte, M. A.; Rubiralta, M.; Diez, A. *J. Org. Chem.* **2001**, *65*, 6992−6999.
(21) Hinds, M. G.; Richards, N. G. J.; Robinson, J. A. *J. Chem. Soc.* **1988**, *1447*, 131−134.
(22) Freidinger, R. M.; Perlow, D. S.; Veber, D. F. *J. Org. Chem.* **1982**, *47*, 104−109.
(23) Kemp, D. S.; McNamara, P. E. *J. Org. Chem.* **1985**, *50*, 5834−5838.
(24) Souers, A. J.; Virgilio, A. A.; Rosenquist, A.; Fenuik, W.; Ellman, J. A. *J. Am. Chem. Soc.* **1999**, *121*, 1817−1825.
(25) Ripka, W. C.; DeLucca, G. V.; Bach, A. C., II; Pottorf, R. S.; Blaney, J. M. *Tetrahedron* **1993**, 3593−3608.
(26) Gardner, B.; Nakanishi, H.; Kahn, M. *Tetrahedron* **1993**, *49*, 3433−3448.
(27) Graf von Roedern, E.; Lohof, E.; Hessler, G.; Hoffmann, M.; Kessler, H. *J. Am. Chem. Soc.* **1996**, *118*, 10156−10167.
(28) Mierke, D. F.; Geyer, A.; Kessler, H. *Int. J. Pept. Protein Res.* **1994**, *44*, 325−31.

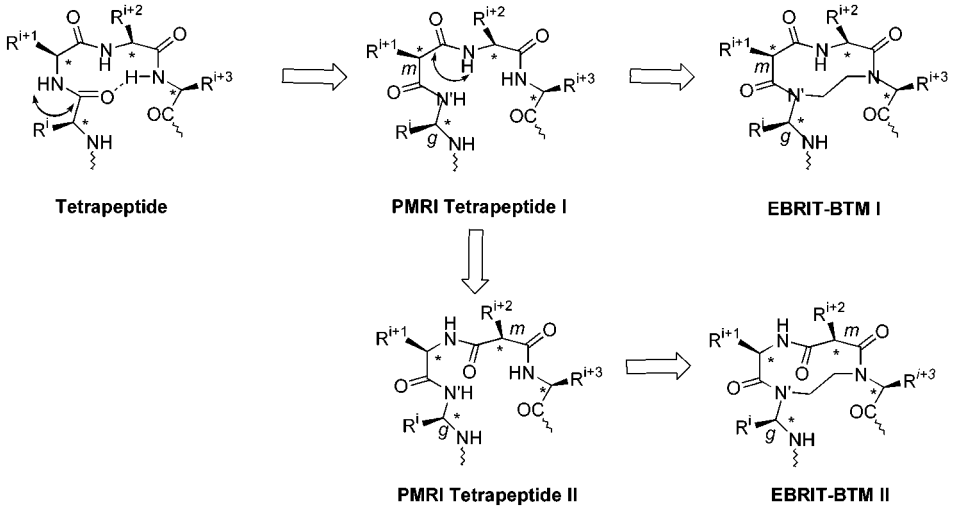

FIGURE 2. Schematics of the structural transformations relating a tetrapeptide to an ethylene-bridged partially modified retro-inverso β-turn mimetic (EBRIT-BTM). Sequential singular retro-inverso transformation of CO_iNH_{i+1} followed by $Co_{i+1}NH_{i+2}$ generates partially modified retro-inverso tetrapeptides **I** and **II** (PMRI tetrapeptides **I** and **II**), respectively. Introduction of an ethylene bridge between N'_i and N_{i+3} transforms PMRI tetrapeptides **I** and **II** into the corresponding EBRIT-BTMs **I** and **II**.

An ideal β-turn mimetic should be a modular unit, in which the characteristics of the critical side chains are maintained. In addition, it should carry amino- and carboxyl-functions, which will allow its incorporation as a synthon into a peptide chain of choice. Moreover, it should allow the presentation of a wide array of side chains in positions *i*-to-*i* + 3. Ideally, the β-turn mimetic should resemble closely the backbone of the turn, reproduce closely the side chain topology, and be devoid of excessive bulk and/or hydrophobicity. Most importantly, the tetrapeptide-like β-turn mimetic should be constructed from readily available building blocks. We also believe that divergence from the perfect topologic mimicry should be compensated by building in sufficient flexibility to allow subtle adjustments to adapt to specific macromolecular targets.

To this end, we report the design, synthesis, and conformational analysis of novel N_i-to-N_{i+3}-ethylene-bridged partially modified retro-inverso tetrapeptide β-turn mimetics (EBRIT-BTM).[31−33] This design applies a minimalistic structural modification approach and fulfills very closely the above criteria for a tetrapeptide-based β-turn mimetic. This tetrapeptide mimetic incorporates a reversal of only a single peptide bond, namely, the $C_iO\cdots N_{i+1}H$ amide bond, and therefore represents a partial retro-inverso modification.[31,32] The EBRIT-BTM structures, H$_2$N-*r*Phe*N*-*m*Gly-Asp-*N*Gly-OH (**16**) and the H$_2$N-*r*Phe-to-Ac-*g*Phe-rearranged Ac-*g*Phe*N*-*m*Gly-Asp-*N*Gly-OH (**18**) (*g*, *gem*-diaminoalkyl; *m*, malonyl; and *r*, direction-reversed amino acid residue) (see Scheme 5), were characterized by proton and carbon NMR and refined with metric-matrix distance geometry (DG) and extensive molecular dynamics (MD) simulations. The salient structural features of the peptidomimetics with respect to their use as molecular scaffolds are presented.

Results and Discussion

Design of the Model N_i-to-N_{i+3}-Ethylene-Bridged Partially Modified Retro-Inverso β-Turn Tetrapeptide Mimetic. Our design sought to transform the putative transient hydrogen-bonded 10-membered ring, characteristic of many β-turn structures, into a 10-membered monoheterocyclic ring. We were committed to maintain the polar nature of the backbone, the characteristic side chains, and their chiral disposition and to accomplish all of the above by employing readily available amino acid derivatives as starting materials. To this end, we utilized the well-established retro-inverso pseudopeptide approach, in which reversal of the amide bond direction in the nonpalindromic backbone is accompanied by the inversion of chiralities at the Cα carbons.[31−33] Specifically, we employed the partial retro-inverso modification in which reversal of a single peptide bond within a sequence, for example, the $C_iO-N_{i+1}H$ amide bond, generates a partially modified retro-inverso peptide (Figure 2, PMRI Tetrapeptide I).[31,32] This partial retro-inverso transformation requires the conversion of the *i*th amino acid residue into the corresponding *gem*-diaminoalkyl residue and the replacement of amino acid residue in position *i* + 1 with a 2-alkyl malonyl residue. In principle, this partial retro-inverso transformation can be extended to the adjacent amide bond, $C_{i+1}O-N_{i+2}H$, reversal of which will result in the incorporation, in the reversed sense of direction, of the enantiomeric form of amino acid residue *i* + 1 and the replacement of amino acid residue *i* + 2 with the corresponding 2-alkyl malonyl moiety (Figure 2, PMRI Tetrapeptide II). Introduction of the *gem*-diamino alkyl in the *i*th position presents N'_i as a potential site for N-alkylation. Therefore, it allows the replacement of the original $C_i{=}O\cdots HN_{i+3}$ hydrogen bond with an $N'_i-CH_2-CH_2-N_{i+3}$ ethylene bridge thus locking a 10-membered heterocyclic ring as a potential

(29) Pellegrini, M.; Royo, M.; Chorev, M.; Mierke, D. F. *J. Pept. Res.* **1997**, *49*, 404−414.
(30) Porcelli, M.; Casu, M.; Lai, A.; Saba, G.; Pinori, M.; Cappelletti, S.; Mascagni, P. *Biopolymers* **1999**, *50*, 211−9.
(31) Goodman, M.; Chorev, M. *Acc. Chem. Res.* **1979**, *12*, 1−7.
(32) Chorev, M.; Goodman, M. *Acc. Chem. Res.* **1993**, *26*, 266−273.
(33) Fletcher, M. D.; Campbell, M. M. *Chem. Rev.* **1998**, *98*, 763−795.

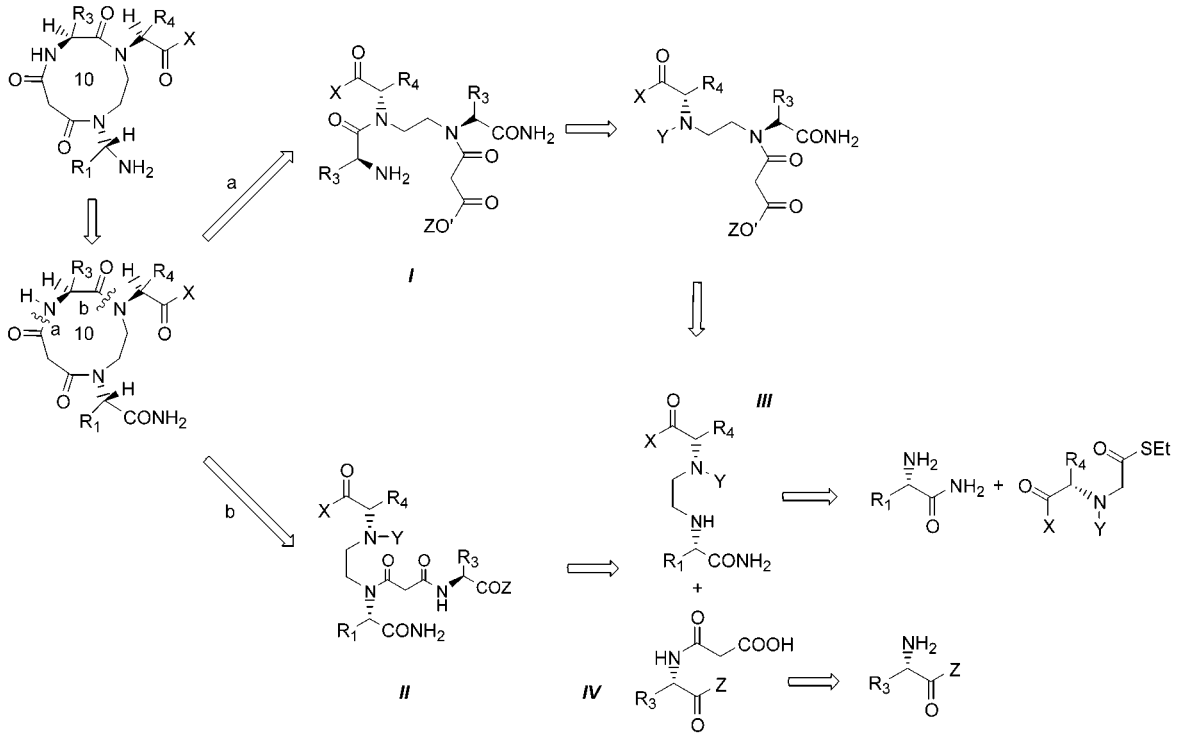

FIGURE 3. Retrosynthesis of ethylene-bridged partially modified retro-inverso β-turn tetrapeptide mimetic **I** (EBRIT-BTM **I**). Pathways **a** and **b** represent synthetic strategies in which ring closure of linear precursors is carried out either between residues $i + 1$ and $i + 2$ of the (2 + 2) partially modified retro-inverso ethylene-bridged tetrapeptide **I** or between residues $i + 2$ and $i + 3$ of the (1 + 3) partially modified retro-inverso ethylene-bridged tetrapeptide **II**, respectively. Both pathways share a common (1 + 1) ethylene-bridged dipeptide **III** [(1 + 1)EB-dipeptide].

ethylene-bridged PMRI tetrapeptide β-turn mimetic (Figure 2, EBRIT-BTM I). In this paper, we report the synthesis of a model EBRIT-BTM I system, Ac-NHCH-(Bzl)N-*m*Gly-Asp-N-CH_2-CO_2H (**18**), which is structurally related to the linear PMRI tetrapeptide Ac-*g*Phe-*m*Gly-Asp-Gly-OH[1].

Synthesis of Model EBRIT-BTM I. Our retrosynthetic analysis, outlined in Figure 3, requires the construction of the linear precursors **I** or **II**, which differ in the designated site for ring closure. End-to-end cyclization of these linear PMRI-ethylene-bridged (EB) tetrapeptides **I** and **II** by forming either peptide bond **a** or **b**, respectively, will accomplish the synthesis of the trisubstituted 2,5,7-trioxo-1,4,8-triazadecane as the EBRIT-I. Intuitively, macrocyclization via pathway **a**, generating a new secondary amide bond between the malonyl residue and the amino acyl moiety, should be easier to carry out than the ring closure via pathway **b**, which generates a tertiary amide bond between an N-alkylated ethylene amino acyl moiety and the carboxyl of an N-acylated amino acid residue. In addition, while pathway **a** represents stepwise addition of monomeric units leading to the assembly of the (2 + 2)PMRI-EB-tetrapeptide **I**, pathway **b** represents a convergent synthesis in which a pseudodipeptide **IV** is condensed with a (1 + 1)EB-dipeptide **III** to generate the (1 + 3)PMRI-EB-tetrapeptide **II**. In both pathways, the reductive alkylations generating the N'_i−CH_2−CH_2−N_{i+3} ethylene bridge comprise the key steps in the synthesis. Both syntheses utilize readily available protected amino acid derivatives as building blocks for the construction of the linear PMRI tetrapeptides **I** or **II**.

SCHEME 1. Preparation of *N*-(*tert*-Butoxycarbonylmethyl)-*N*-Fmoc *S*-Ethyl Thioglycinate (4)[a]

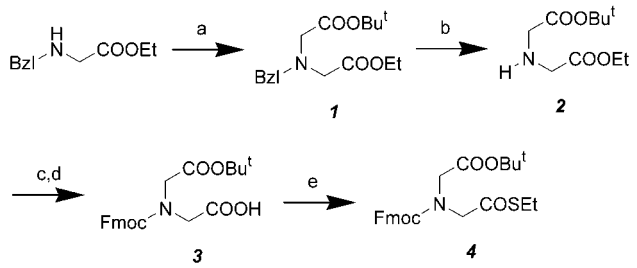

[a] Reaction conditions: (a) *tert*-butyl bromoacetate, K_2CO_3, in DMF, 95 °C, 4 h, 86%; (b) 10% Pd−C, H_2 in 95% EtOH, 40 psi, 2 h, 97%; (c) LiOH in dioxane−H_2O, 4°C, overnight; (d) Fmoc-Cl, $NaHCO_3$, room temperature, 4 h, 86%; (e) EtSH, DCC, DMAP in DCM, room temperature, 2 h, 87%.

The first building block for pathways **a** and **b** is *N*-(*tert*-butyloxycarbonylmethyl)-*N*-Fmoc *S*-ethyl thioglycinate (**4**), which was obtained in an overall yield of 62% (Scheme 1). Alkylation of ethyl *N*-benzyl glycinate by *tert*-butyl bromoacetate yielded the orthogonally protected ethyl *tert*-butyl *N*-benzyliminoacetate **1** that was further manipulated to yield the free acid **3**. DCC-mediated thioesterification of **3** with ethanethiol[35] generated the thioester **4** in 87% yield.

(34) Bergmeier, S. C.; Cobas, A. A.; Rapoport, H. *J. Org. Chem.* **1993**, *58*, 2369−2376.

SCHEME 2. Building the Ethylene Bridge through Reductive Alkylation

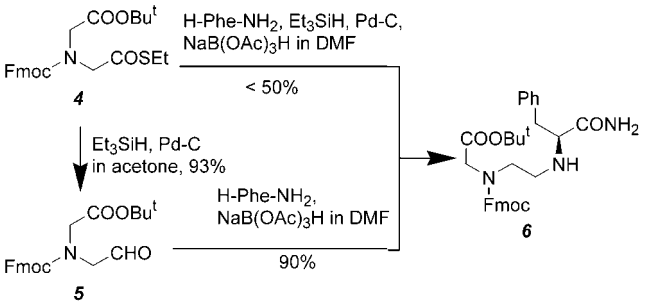

The (1 + 1)EB-dipeptide **6** (Scheme 2) is the common intermediate for pathways **a** and **b** represented by compound **III** in the retrosynthetic scheme (Figure 3). Alternative approaches to prepare *N*-(*tert*-butoxycarbonylmethyl)-*N*-Fmoc *S*-ethyl thioacetate (**4**) failed. These included attempts to ring-open *N*-Fmoc-iminodiacetic acid anhydride[34] with either *tert*-butyl alcohol or ethanethiol and to N-alkylate *tert*-butyl glycinate with benzyl bromoacetate in the presence of K_2CO_3 and tetrabutylammonium hydrogensulfate (TBA).

The formation of the $N'_i-CH_2-CH_2-N_{i+3}$ ethylene bridge in **6** was accomplished by a two-step procedure,[35−37] which was found to be superior to our previously published one-pot reductive alkylation.[38] In the first step, thioglycinate **4** was reduced to the corresponding aldehyde **5** in 93% yield. Due to the limited stability of aldehyde **5** at room temperature, it was used shortly after synthesis. In the following step, sodium triacetoxyborohydride [$NaB(OAc)_3H$]-mediated reductive alkylation of phenylalaninamide with the aldehyde **5** generated the ethylene-bridged intermediate in 90% yield, bringing the total yield of this procedure to about 84%.[38,39] In comparison, the one-pot reductive alkylation procedure yielded less than 50% of the ethylene-bridged compound **6**.[38]

Pathway **b** represents a convergent synthesis in which a pseudodipeptide **IV** is coupled to a (1 + 1)EB-dipeptide **III** to yield the linear (1 + 3)EB-tetrapeptide **II**, the precursor for the final macrocyclization (Figure 3). The synthesis of fully protected model β-turn mimetic pseudodipeptide *N*-(*tert*-butyloxycarbonylmethylcarbonyl) α-(9-fluorenylmethyl) and β-cyclohexyl L-aspartate (*tert*-butyl *m*Gly-Asp(OcHex)OFm) (**7**) and its partially protected form **8** are outlined in Scheme 3.

The *O*-(7-azabenzotriazole-1-yl)-1,1,3,3-tetramethyluronium hexafluorophosphate (HATU)[40,41]-mediated coupling between the secondary amine in the (1 + 1)EB-dipeptide **6** and the PMRI dipeptide HO-*m*Gly-Asp-(OcHex)-OFm (**8**) generated the fully protected linear (1 + 3)EB-tetrapeptide partially deprotected **9**, in 92% yield (Scheme 4). However, macrocyclization carried out by dropwise addition of **9** in the deprotection mixture that

SCHEME 3. Preparation of *N*-Malonyl α-(9-Fluorenylmethyl)-β-cyclohexyl Aspartate[a]

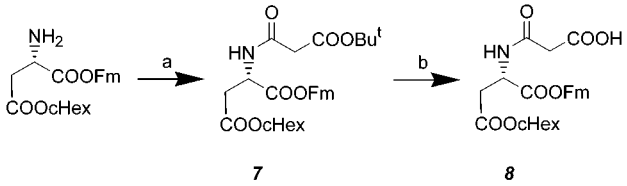

[a] Reaction conditions: (a) $HOOCCH_2COOBu^t$, DCC in DCM, room temperature, 2 h, 92%; (b) saturated HCl in Et_2O, room temperature, overnight, 100%.

SCHEME 4. Synthesis of Model ERBIT-BTM via Pathway a Applying 2 + 2 Fragment Condensation

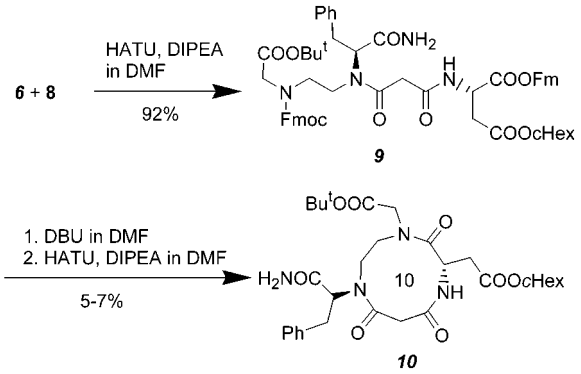

removed the *N*-Fmoc/OFm protecting groups (1 equiv of 1,8-diazabicyclo[5,4,0]undec-7-ene (DBU) in dimethylformamide (DMF)) to a solution of HATU and DIPEA in DMF generated a very complicated reaction mixture. LC−ESIMS analysis of this mixture revealed that intramolecular coupling occurred to a very limited extent and the anticipated fully protected model EBRIT-BTM **10** was only a minor product (5−7% yield) (Scheme 4). Attempts to carry out this macrocyclization in a highly diluted solution[42] yielded similarly disappointing results. This apparently difficult intramolecular coupling is caused by a combination of the low reactivity of the secondary amine, the steric hindrance imposed by the *N*-*tert*-butyloxycarbonylmethyl substituent on the secondary amine, and the structural strain involved in the ring closure to obtain the 2,5,7-trioxo-1,4,8-triazadecane system.

The alternative synthetic pathway **a** employed the same (1 + 1)EB-dipeptide **6** used in pathway **b**, which is extended by the monomeric units in a stepwise manner (Scheme 5). The overall yield of the fully protected (2 + 2)EB-tetrapeptide **13** after two HATU-mediated couplings and an intervening DBU-mediated deprotection of the *N*-Fmoc from the secondary amine in the (1 + 2)-EB-tripeptide **11** was 71%. Catalytic hydrogenation of **13** in which *N*-Cbz and *O*-Bzl protecting groups were quantitatively removed generated the partially protected linear (2 + 2)EB-tetrapeptide **14**. Importantly, the linear precursor was labile upon storage. After several days at room temperature, it spontaneously cyclized to the corresponding diketopiperazine **15** as confirmed by LC−ESIMS and ^{1}H NMR (data not shown). HATU-mediated

(35) Kim, H. O.; Ji, X. D.; Melman, N.; Olah, M. E.; Stiles, G. L.; Jacobson, K. A. *J. Med. Chem.* **1994**, *37*, 3373−3382.
(36) Fukuyama, T.; Lin, S. C.; Li, L. *J. Am. Chem. Soc.* **1990**, *112*, 7050−7051.
(37) Ho, P. T.; Ngu, K. Y. *J. Org. Chem.* **1993**, *58*, 2313−2316.
(38) Han, Y.; Chorev, M. *J. Org. Chem.* **1999**, *64*, 4, 1972−1978.
(39) Abdel-Magid, A. F.; Carson, K. G.; Harris, B. D.; Maryanoff, C. A.; Shah, R. D. *J. Org. Chem.* **1996**, *61*, 3849−3862.
(40) Carpino, L. A. *J. Am. Chem. Soc.* **1993**, *115*, 4397−4398.
(41) Carpino, L. A.; El-Faham, A. *J. Org. Chem.* **1994**, *59*, 695−698.
(42) Weitz, I. S.; Pellegrini, M.; Mierke, D. F.; Chorev, M. *J. Org. Chem.* **1997**, *62*, 2527−2534.

SCHEME 5. Synthesis of Model ERBIT-BTM Compounds

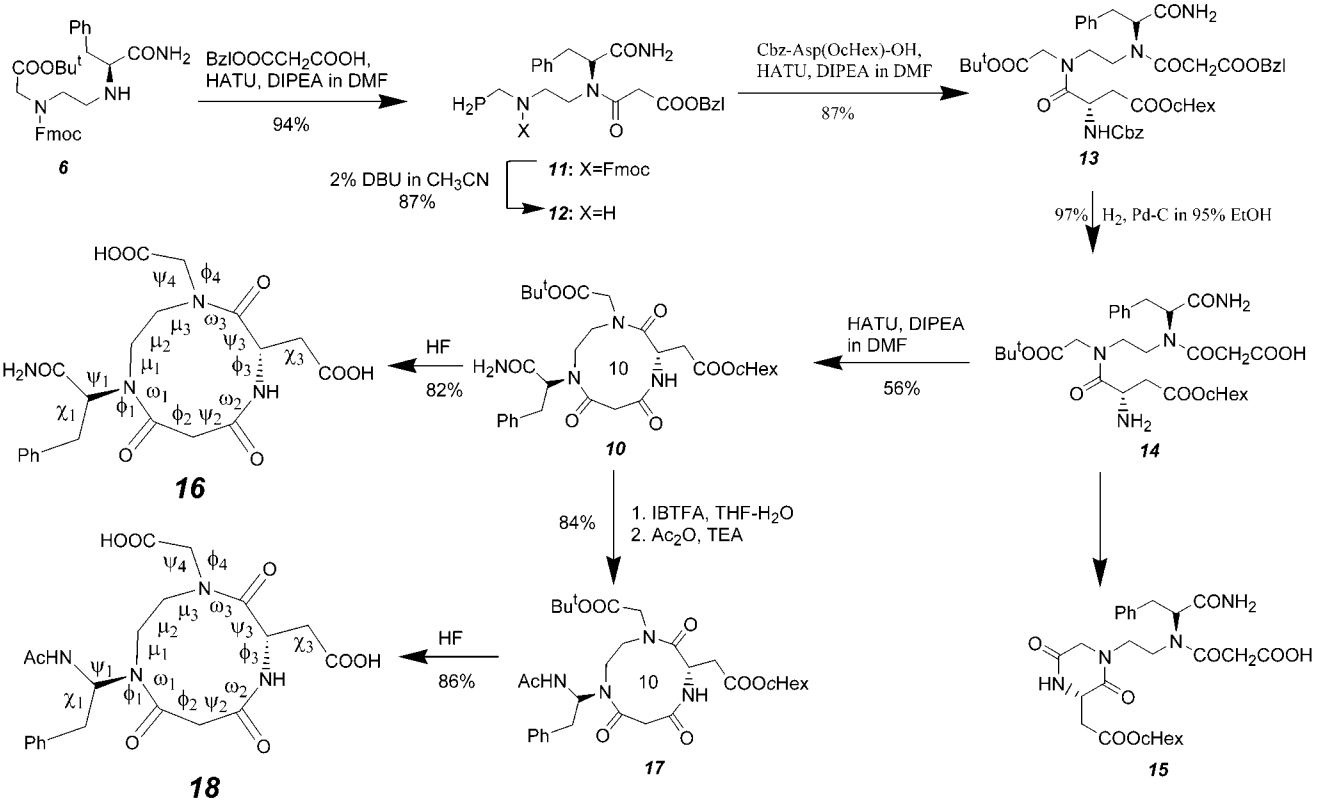

cyclization of **14** generated a new secondary amide bond between a carboxyl of the malonyl residue and a free amino of the aspartic acid at a yield of 56%. The yield of the fully protected ERBIT-BTM **10**, obtained through pathway **a**, was 8 to 11-fold higher than the one obtained via pathway **b**. Intermolecular coupling was effectively overcome by the slow dropwise addition (>2 h) of the DMF solution of **14** to the solution containing the coupling reagent. Removal of the side chain protecting groups, *O*-cHex and *O*-Bu^t, from **10** was carried out in liquid HF at 0 °C and generated the model ERBIT-BTM **16** in 82% yield.

The presence of the carboxamide function at the amino acid residue in the *i*th position of the ERBIT-BTM **10** was aimed at allowing the conversion of this residue into the corresponding *gem*-diaminoalkyl by a mild oxidative Hofmann-type rearrangement with iodobenzene bis-(trifluoroacetate) (IBTFA) in aqueous solution.[43] The introduction of the *gem*-diaminoalkyl residue offers the opportunity to resume chain elongation toward the amino-terminus with the backbone recovering the correct sense of direction. The rearrangement reaction was very fast and efficient, and the generated product was stable in the reaction mixture for several hours (as monitored by LC−ESIMS). Long-term stabilization was achieved by acetylation of the free amino group in the *gem*-diaminoalkyl moiety, generating the N'_i-to-N_{i+3} ERBIT-BTM Ac-*g*PheN-*m*Gly-Asp(OcHex)-NGly-OBu^t (**17**). Final removal of the *O*-Bu^t and *O*-cHex protecting group is accomplished in liquid HF generating the model N'_i-to-N_{i+3} ERBIT-BTM Ac-*g*PheN-*m*Gly-Asp-NGly-OH (**18**) in 86% yield.

A closely related approach to synthesize a γ-turn mimetic, as a fibrinogen receptor antagonist, was reported by Callahan et al.[44] (Figure 4). Reversal of the *i*-to-*i* + 1 amide bond followed by ethylene bridging of N_i-to-N_{i+2} yielded a seven-membered PMRI γ-turn mimetic. The major shortcoming of this design is the absence of a carboxyl function that will allow the extension of the main chain with a C-terminus sequence, and the method therefore does not generate a synthon that can be incorporated as a γ-turn mimetic building block within a sequence. The use of an ethylene-bridged constraint was reported as a means to link N_i and N_{i+1} generating 2-oxopiperazines as dipeptidomimetics (Figure 4).[45] However, this conformationally constrained system was not designed to mimic a known element of secondary structure.

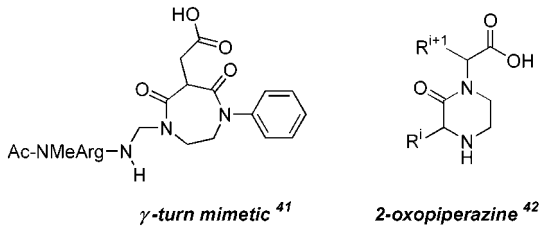

FIGURE 4. Examples of ethylene-bridged peptidomimetics reported in the literature. In these structures, the bridging is either N_i-to-N_{i+2} or N_i-to-N_{i+1}.

(43) Radhakrishna, S. A.; Parham, M. E.; Riggs, R. M.; Loudon, G. M. *J. Org. Chem.* **1979**, *44*, 1746−1747.

(44) Callahan, J. F.; Newlander, K. A.; Brugess, J. L.; Eggleston, D. S.; Nichols, A.; Wong, A.; Huffman, W. F. *Tetrahedron* **1993**, 3479−3488.

TABLE 1. ^{1}H and ^{13}C Chemical Shifts (ppm, relative to TMS) of Model EBRIT-BTM Structures

		16				**18**			
		H		^{13}C	^{13}C=O	H		^{13}C	^{13}C=O
Ac	HN					8.37			170.0
	CH_3					1.79		22.7	
Phe	α	4.64		60.5	171.3	5.74		62.1	
	β	3.05[a]	3.23	34.3		2.76[a]	2.82[a]	39.2	
*m*Gly	α	3.11	3.73[a]	45.4	166.8, 167.8	3.05	3.71	45.8	165.1, 167.5
Asp	HN	9.04				9.02			
	α	5.01		47.4	170.2	5.08		47.7	171.3
	β	2.33	2.66	36.1	171.5	2.36	2.71[a]	36.2	172.5
Gly	α	3.74[a]	3.94	48.9	169.8	3.82	4.03	49.2	173.2
Ac	HN					8.37			170.0
	CH_3					1.79		22.7	
Eth	C1	3.06[a]	3.26[a]	46.6		3.11	3.56[a]	46.9	
	C2	3.26[a]	3.55	46.8		3.49[a]	3.64	42.3	

[a] Overlapped resonances.

TABLE 2. Experimental Distances in Model EBRIT-BTM Structures Derived from ROESY Spectra[a,b]

cross peaks		distance (Å)		cross peaks		distance (Å)	
		16	**18**			**16**	**18**
Phe Hα	Phe H*βR*	3.3	2.6*	Asp HN	Eth H2*R*	2.6	2.6
Phe Hα	Phe H*βS*	2.7	3.0*	Asp HN	Eth H2*S*	3.6	3.9
Phe Hα	Phe H*γ*	3.7		Asp Hα	Asp H*βR*	2.7	2.5*
Phe Hα	Ac HN		3.2	Asp Hα	Asp H*βS*	2.3	2.4*
Phe Hα	Eth H2*R*		3.4	Asp Hα	*m*Gly H*αR*	3.3	
Phe Hα	Eth H2*S*		2.6	Asp Hα	Eth H1*R*		2.0
Phe H*βR*	Phe H*γ*	3.4	4.1*	Asp Hα	Eth H1*S*	3.0	
Phe H*βR*	Ac HN		3.2*	Gly H*αR*	Eth H1*R*	3.3	
Phe H*βR*	Eth H1*S*		4.0*	Gly H*αR*	Eth H2*R*	2.2	3.3
Phe H*βS*	Eth H1*S*		3.6*	Gly H*αR*	Eth H1*S*	2.8	3.2
Phe H*βS*	Phe H*γ*	3.4	4.1*	Gly H*αS*	Asp Hα	2.7	
*m*Gly H*αS*	Eth H2*R*		2.2	Gly H*αS*	Eth H1*R*	2.8	
*m*Gly H*αS*	Eth H2*S*		3.8	Gly H*αS*	Eth H1*S*	2.9	2.7
Asp HN	Asp Hα	2.9	3.0	Ac HN	Eth H2*S*		2.6
Asp HN	Asp H*βR*	3.3	3.5*	Ac HN	Ac CH_3		3.5
Asp HN	Asp H*βS*	3.0	3.1*	Eth H1*R*	Eth H2*R*	2.2	
Asp HN	*m*Gly H*αS*	2.2	2.3				

[a] *R* and *S* indicate pro-*R* and pro-*S* stereospecific assignments, respectively. [b] Asterisk indicates nonstereospecific assignment.

TABLE 3. ^3J Proton−Proton Coupling Constants (Hz) in the Model EBRIT-BTM Structures Obtained from PE-COSY Spectra[a,b]

	16	**18**
Phe Hα−Phe H*βR*	8.4	
Phe Hα−Phe H*βS*	6.4	
Asp HN−Asp Hα	9.6	10.0
Asp Hα−Asp H*βR*	9.2	8.4*
Asp Hα−Asp H*βS*	3.6	4.4*
Eth H1*S*−Eth H2*R*	7.6	
Eth H1*R*−Eth H2*R*	1.2	
Eth H1*S*−Eth H2*S*	8.2	
Eth H1*R*−Eth H2*S*		

[a] *R* and *S* indicate pro-*R* and pro-*S* stereospecific assignments, respectively. [b] Asterisk indicates nonstereospecific assignment.

Conformational Analysis. The ^{1}H and ^{13}C NMR spectra display one complete set of signals for each peptide mimetic, indicating the lack of cis/trans isomerization about the amide bonds. The ^{1}H and ^{13}C chemical shifts obtained from total-correlation spectroscopy (TOCSY), ^{1}H−^{13}C heteronuclear multiple-quantum shift correlation (HMQC), and heteronuclear multiple bond connectivity (HMBC) spectra are provided in Table 1. Nuclear Overhauser enhancement spectroscopy (NOESY) spectra yielded very few structurally informative cross-peaks, as would be expected for a molecule of this size in dimethyl sulfoxide (DMSO) at 298 K. All distance restraints were generated from two-dimensional rotating frame NOE spectroscopy (ROESY) spectra (Table 2). The $^3J_{HH}$ coupling constants obtained from primitive exclusive correlation spectroscopy (PE-COSY) spectra are provided in Table 3. These coupling constants were used along with the HMBC long-range heteronuclear couplings for the diastereotopic assignment of the *β*-protons of Asp and *r*Phe of **16**. Overlapped ^{13}C resonances between the amide carbon and the carboxyl carbon of Asp precluded the stereospecific assignment of the Asp *β* protons of **18**.

Random metrization and distance- and angle-derived dynamics (DADD) simulations utilizing two-dimensional rotating frame NOE (ROE) restraints produced 95−100 conformations with small violations (less than 0.3 Å for ROEs). With the exception of the backbone dihedral angles of *r*,*g*Phe (ϕ_1 and ψ_1), the dihedral angles of **16** and **18** populated the same conformational space. The three amide bonds in the 10-membered ring were preferentially oriented in the trans configuration, and the projecting *r*,*g*Phe, Asp, and Gly residues displayed varying degrees of conformational freedom. A comparison of the ϕ_1 and ψ_1 dihedral angles of *r*Phe and *g*Phe revealed marked differences in their conformational preference (Figure 5). The ϕ_1 and ψ_1 dihedral angles of *r*Phe were dispersed, as expected for this exo-cyclic residue, while the corresponding dihedral angles of *g*Phe were tightly clustered. Within the cyclic ring system, the ϕ_2 and ψ_2 dihedral angles of *m*Gly of both compounds were more dispersed than the other ϕ,ψ pairs.

The conformations of the DG structures were analyzed, and a structure that was representative of the distribution of dihedral angles, energies, and distance restraint violations was selected for each mimetic and further refined using EM and MD simulations (Figures 6 and 7). The DG algorithm generated structures that satisfied the experimentally derived and holonomic distance restraints without regard for intra- and intermolecular interactions (e.g., partial charges, Coulombic interactions,

(45) (a) DiMaio J.; Bernard, B. *J. Chem. Soc., Perkin Trans. 1* **1989**, 1687−1689. (b) Kojima, Y.; Ikeda, Y.; Kumata, E.; Maruo, J.; Okamoto, A.; Hirostu, K.; Shibata, K.; Ohsuka, A. *Int. J. Pept. Protein Res.* **1991**, *37*, 468−475. (c) Pohmann, A.; Schanen, V.; Guillaume, D.; Quirion, J.-C.; Husson, H.-P. *J. Org. Chem.* **1997**, *62*, 1016−1022.

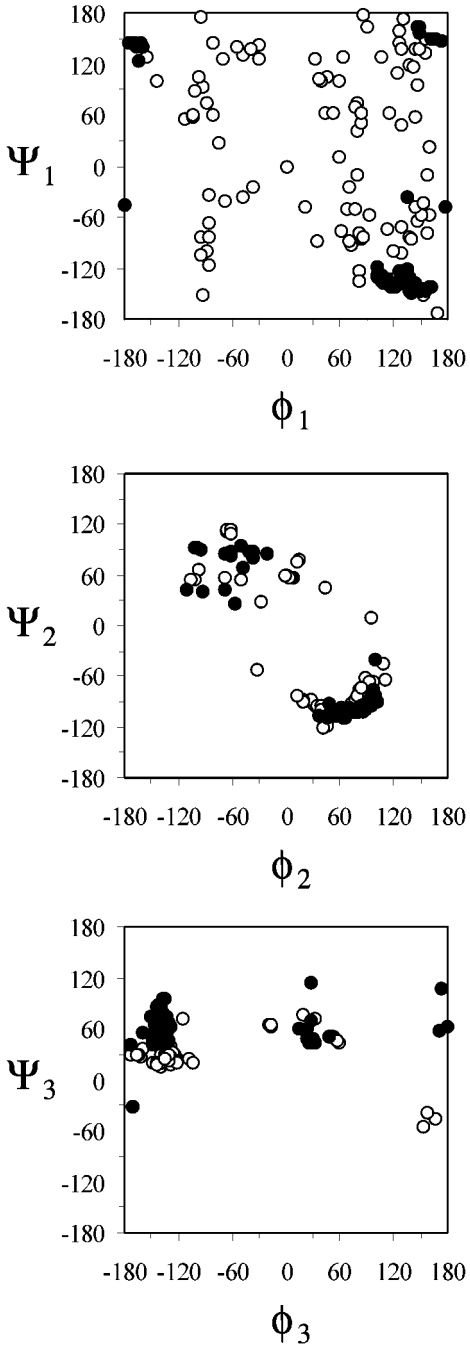

FIGURE 5. Ramanchandran plots indicating the conformational space of the ϕ_1 and ψ_1 of *r*,*g*Phe, the ϕ_2 and ψ_2 of *m*Gly, and the ϕ_3 and ψ_3 of Asp, during the DG simulation. Open (○) and closed (●) circles depict dihedral angle pairs for structures **16** and **18**, respectively.

and Lennard−Jones interactions). Through the use of restrained EM and MD simulations, the conformational space of the EBRIT-BTM scaffolds with respect to the potential energy surface was assessed in DMSO, the same solvent system that was used in the NMR experiments. The dihedral angles of the representative energy-minimized structures of EBRIT-BTM **16** and **18** were consistent between the two structures (Table 4). During the MD simulation, the backbone atoms of the core 10-membered ring system did not undergo major conformational changes, as illustrated by the superposition of structures taken from the MD trajectory (Figure 7).

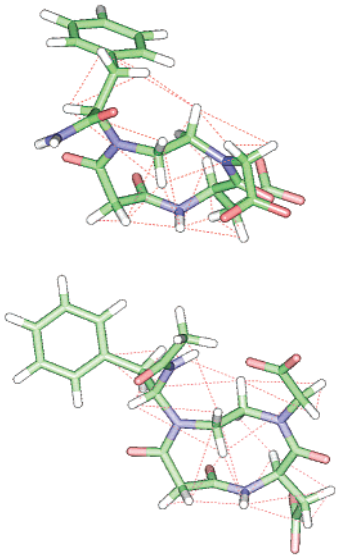

FIGURE 6. Energy-minimized structures of model EBRIT-BTM H_2N-*r*Phe*N*-*m*Gly-Asp-*N*Gly-OH **16** (top) and Ac-*g*Phe-*N*-*m*Gly-Asp-*N*Gly-OH **18** (bottom) in DMSO. ROEs are indicated by dashed lines.

The ring structures of EBRIT-BTMs **16** and **18** were derived from ethylene-mediated cyclization of the amide nitrogens of *r*Phe$_i$ and Gly$_{i+3}$. Cyclization of the peptide mimetics resulted in a constrained ring system with a limited number of conformations. As anticipated, the structures of the 10-membered ring system for EBRIT-BTM **16** and **18** were nearly identical (Table 4). The results from the MD simulations also indicate a low degree of flexibility in the core ring system (Figure 7), a desirable feature for maintaining the optimal topological display of the pharmacophores. As expected, the side chains, with unhindered rotation about the Cα−Cβ bonds, displayed a much higher degree of flexibility.

Superposition of the heavy backbone atoms of the 10-membered ring, excluding the ethylene bridge, with the standard β-turn structures (Figure 8) indicated that the EBRIT-BTM system most closely resembled a type II′ β-turn (RMSD 0.3 Å). Superposition of compound **18** with a model βII′-turn (ϕ,ψ values of +60°, −120°, −80°, and 0°) is illustrated in Figure 8. The distances between the Cα$_i$ and Cα$_{i+3}$ atoms of the model EBRIT-BTM **II**, namely, compound **18** (5.5 Å), and the βII′-turn (5.1 Å) were comparable, indicating a propensity for the β-turn mimetic to nucleate the formation of a β-sheet.

Rearrangement of the carboxamide group −CONH$_2$ in **16** and concomitant acetylation transformed it into the acetamido group −NHCOCH$_3$ (compound **18**). This modification resulted in the formation of an intramolecular hydrogen bond between the NαH of *g*Phe-COCH$_3$ and the carboxyl of Gly, as observed by the DG, EM, and MD calculations. The distance between the hydrogen bond donor and the acceptor was 2.2 Å, and the distance between the nitrogen and oxygen atoms was 2.9 Å. This hydrogen bond is consistent with the onset of an antiparallel β-sheet. The model EBRIT-BTM **18** mimics the β-turn often found at the center of an antiparallel β-sheet,

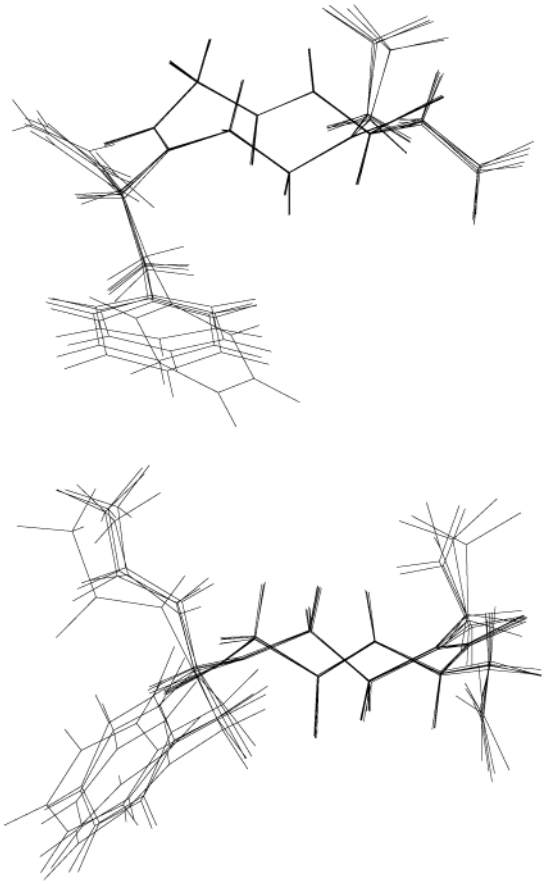

FIGURE 7. Results from the molecular dynamics simulations of model EBRIT-BTM H_2N-*r*Phe*N*-*m*Gly-Asp-*N*Gly-OH **16** (top) and Ac-*g*Phe*N*-*m*Gly-Asp-*N*Gly-OH **18** (bottom) in DMSO. Molecules have been superimposed using the heavy backbone atoms of the ring system. The degree of overlap among the structures is indicative of the conformational flexibility in the system.

TABLE 4. Dihedral Angles of Model EBRIT-BTM Structures 16 and 18 Following Energy Minimization of Selected DG Structures

	16	18		16	18
ϕ_1	−111	−166	ψ_3	63	65
ψ_1	−89	105	χ_3	−172	−75
χ_1	−71	−145	ω_3	−169	173
ω_1	170	174	ϕ_4	55	159
ϕ_2	79	60	μ_1	−91	−97
ψ_2	−118	−116	μ_2	153	166
ω_2	141	149	μ_3	−112	−92
ϕ_3	−122	−113			

and with the correct orientation of the attached amide and carbonyl groups, the second hydrogen bond is formed. Therefore, compound **18** may find use in the stabilization of β-sheets. In contrast, compound **16** without the ability to form this hydrogen bond, although it maintains the correct overall topology of a β-turn, does not stabilize the propagation of a β-sheet. The stabilization provided by this exo-cyclic hydrogen bond can be seen in the ϕ,ψ dihedral angles of Phe (Figure 5).

Recently, a conformationally constrained β-sheet mimetic was shown to inhibit dimerization of human immunodeficiency virus type 1 protease, a homodimeric protein consisting of two subunits linked through a two-stranded antiparallel β-sheet.[46] Therefore, in addition to providing a structural role, β-turn mimetics may potentially provide a functional role as well. The EBRIT-BTM scaffolds and their structural features as determined here will greatly assist in these efforts.

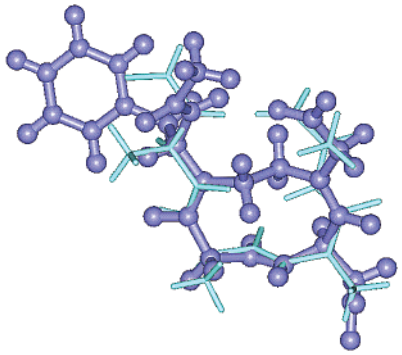

FIGURE 8. Superposition of the heavy backbone atoms of the 10-membered ring system of model EBRIT-BTM Ac-*g*Phe*N*-*m*Gly-Asp-*N*Gly-OH (**18**) with the amino acid residues of an ideal βII′ turn.

Conclusion

The design, synthesis, and conformational analysis of novel model EBRIT-BTMs **16** and **18** presented in this report offer new forms of backbone-to-backbone conformational constraints. This approach not only spares the integrity of the original side chains and maintains the overall polar nature of the backbone but also avoids the introduction of extra bulky and hydrophobic aromatic or aliphatic ring moieties. The lack of these extra structural features eliminates sites that may contribute to nonspecific interactions at the macromolecular acceptor and compromise solubility. The design and synthesis employ readily available building blocks and allow a large degree of diversification that includes the choice of the peptide bond reversal site and the selection of side chains and chirality at the Cα-carbons comprising the ring. The EBRIT-BTM can be used either in isolation as a molecular scaffold to present pharmacophores of choice at a restricted topology, or as a conformational element mimetic when incorporated into peptide sequences. Evidently, the model EBRIT-BTM compounds **16** and **18** include achiral residues in positions $i+1$ and $i+3$, *m*Gly and Gly, respectively. We believe that the methodology described in this report will generate the EBRIT-BTM compounds containing chiral residues at these positions but probably in a lower overall yield. In addition, incorporating C-2-substituted-malonyl residues may introduce configurational lability at the malonyl chiral carbon, which may lead to enhanced conformational heterogeneity. As previously reported, the configurational lability of the chiral malonyl residue depends on the nature of the C-2 substituent and the nature of the flanking sequences.[31−33] Taken together, these EBRIT-BTM systems offer new tools to investigators interested in elucidating the biologically relevant conformation of

(46) Bouras, A.; Boggetto, N.; Benatalah, Z.; de Rosny, E.; Sicsic, S.; Reboud-Ravaux, M. *J. Med. Chem.* **1999**, *42*, 957−962

peptides and will help molecular designers of peptide-based drugs in their search for smaller, more selective, pharmacokinetically more favorable peptide mimetics.

Our future efforts will be directed to improve and implement the synthetic methodology and expand the diversity of these EBRIT-BTMs. We will also use these systems as molecular scaffolds and as conformational determinants of secondary structure elements to generate peptidomimetics of biological interest.

Experimental Section

General Methods. Thin-layer chromatography (TLC) was performed on plastic plates coated with (0.20 mm) silica gel 60 F254. Open column chromatography was carried out on silica gel 60 (200−400 mesh) using the solvent mixture as indicated for TLC. All organic phases obtained from extraction of aqueous solutions were dried over $MgSO_4$ prior to evaporation in vacuo. Analytical reversed-phase high-performance liquid chromatography (RP-HPLC) was carried out on a Waters 100 RP-18 column (5 μm, 19 mm × 150 mm) column at a flow rate of 1 mL/min. Semipreparative RP-HPLC was carried out on a Vydac 90 Å C-18 column (15−20 μm, 10 × 250 mm) at a flow rate of 20 mL/min. Preparative RP-HPLC was carried out on a Vydac 300 Å C-18 column (15−20 μm, 47 × 300 mm) at a flow rate of 70 mL/min. The solvent system used in RP-HPLC included the following: solvent A, 0.1% (v/v) TFA in H_2O; solvent B, 0.1% TFA in CH_3CN. The effluent was monitored at 220 nm. ^{1}H and ^{13}C NMR spectra were collected on a 500 MHz instrument. NMR chemical shifts are reported in parts per million. ^{1}H chemical shifts were calibrated using tetramethylsilane (TMS) as an internal standard (0 ppm). ^{13}C chemical shifts were calibrated using the $CDCl_3$ resonance (77.2 ppm) or DMSO-d_6 resonance (39.5 ppm) as an internal standard unless otherwise noted. The coupling constants in hertz were determined from the one-dimensional spectra unless otherwise noted. Melting points were determined with a capillary melting point apparatus and are uncorrected. Elementary microchemical analysis was carried out at E+R Microanalytical Laboratory, Inc., NY. Analytical results were within 0.3% of the theoretical values. Mass spectroscopy was performed in our laboratory using an electrospray ionization (ESI) source. *N*,*N*-Dimethylformamide (DMF) was dried with 4 Å molecular sieves for 48 h before use. Other commercially available chemicals were used without further treatment. Monobenzylmalonate[47] and *N*-benzyloxycarbonyl β-cyclohexyl aspartate[48] were prepared according to published procedures.

***N*-Benzyl-*N*-(ethoxycarbonylmethyl)glycine *tert*-Butyl Ester (1).** A mixture of *N*-benzylglycine ethyl ester (19.3 g, 100 mmol), *tert*-butyl bromoacetate (21.4 g, 110 mmol), and K_2CO_3 (13.8 g, 100 mmol) in DMF (100 mL) was heated at 95−100 °C for 4 h and then concentrated in vacuo. The residue was extracted with EtOAc (500 mL), washed with water (2 × 300 mL) and brine (100 mL), dried, and concentrated in vacuo. Purification by flash column chromatography on silica gel afforded 26.4 g of **1** (86% yield) as a colorless oil: R_f = 0.43 (15:85 EtOAc/hexane); R_t = 18.05 min (0−100% B in A 30 min); ^{1}H NMR ($CDCl_3$) δ 7.40−7.30 (m, 5H, ArH), 4.16 (q, 2H, J = 7.3 Hz, CH_2CH_3), 3.91 (s, 2H, CH_2Ph), 3.53 (s, 2H, CH_2-COOBu^t), 3.44 (s, 2H, CH_2COOEt), 1.46 (s, 9H, Bu^t), 1.26 (t, 3H, J = 7.3 Hz, CH_2CH_3); ^{13}C NMR δ 171.3, 170.5, 138.3, 129.2, 128.4, 127.4, 81.1, 60.4, 57.7, 55.1, 54.3, 28.2, 14.3; ESIMS calcd for $C_{17}H_{25}NO_4$ 307.38, found m/z = 308 (M + H)$^+$. Anal. Calcd for $C_{17}H_{25}NO_4$: C, 66.43; H, 8.20; N, 4.56; Found: C, 66.21; H, 8.17; N, 4.74.

***N*-(Ethoxycarbonylmethyl)glycine *tert*-Butyl Ester (2).** A mixture of **1** (21.5 g, 70 mmol) and 10% Pd−C (2 g) in 95% ethanol (200 mL) was hydrogenated at 40 psi for 2 h and then filtered through a Celite bed, concentrated in vacuo, and vacuum-dried to afford 14.9 g of **2** (97% yield) as a colorless oil. This crude product was used in the next step without further purification: R_t = 11.72 min (0−100% B in A, 30 min); ^{1}H NMR ($CDCl_3$) δ 5.76 (broad, 1H), 4.16 (q, J = 7.5 Hz, 2H), 3.46 (s, 2H), 3.36 (s, 2H), 1.46 (s, 9H), 1.26 (t, J = 7.5 Hz, 3H); ^{13}C NMR δ 81.5, 57.3, 56.0, 55.1, 28.2, 14.3; ESIMS calcd for $C_{10}H_{19}NO_4$ 217.26, found m/z = 218 (M + H)$^+$.

***N*-(Carboxymethyl)-*N*-Fmoc-glycine *tert*-Butyl Ester (3).** Compound **2** (13.0 g, 60 mmol) was dissolved in dioxane (200 mL) and cooled with an ice−water bath. $LiOH\cdot H_2O$ (2.94 g, 70 mmol) in water (200 mL) was then added, and the resulting mixture was stirred at 5 °C overnight. Addition of $NaHCO_3$ (5.9 g, 70 mmol) was followed by introduction of small aliquots of Fmoc-Cl (18.1 g, 70 mmol). The resulting mixture was slowly warmed to room temperature and stirred for 6 h and then neutralized with saturated $KHSO_4$ to pH = 3, concentrated in vacuo to ∼300 mL, and extracted with EtOAc (3 × 200 mL). The combined extract was washed with water (200 mL), dried, and concentrated in vacuo. Purification by column chromatography afforded 21.2 g of **3** (86% yield): R_f = 0.43 (35:64:1 EtOAc/hexane/HOAc); ^{1}H NMR ($CDCl_3$) δ (cis/trans isomers) 7.78−7.30 (m, 8H), 4.47 (d, J = 5.5 Hz, 2H), 4.28−4.15 (m, 5H), 4.02 (s, 1H), 3.98 (s, 1H), 1.47 (s, 9H), 1.25 (t, J = 7.5 Hz, 1.5H), 1.24 (t, J = 7.5 Hz, 1.5H); ^{13}C NMR δ (cis/trans isomers) 198.0, 168.5, 156.2, 143.8, 141.4, 128.0, 127.3, 125.2, 120.1, 82.6, 68.6, 57.6, 57.4, 50.6, 50.5, 47.3, 47.2, 28.2, 23.4, 14.4; ESIMS calcd for $C_{23}H_{25}NO_6$ 411.45, found 412 (M + H)$^+$. Anal. Calcd for $C_{23}H_{25}NO_6$: C, 67.14; H, 6.12; N, 3.40. Found: C, 66.96; H, 6.17; N, 3.52.

***N*-(*S*-Ethyl Thiocarbonylmethyl) *N*-Fmoc-Glycine *tert*-Butyl Ester (4).** *N*,*N*′-Dicyclohexylcarbodiimide (DCC) (11.3 g, 55 mmol) was added to an ice-cold solution of **3** (20.5 g, 50 mmol), EtSH (7.7 mL, 100 mmol), and 4-(dimethylamino)-pyridine (630 mg, 5 mmol) in dichloromethane (DCM) stirred at room temperature for 2 h, filtered, concentrated in vacuo, and purified by flash column chromatography to afford 19.5 g of **4** (87% yield) as a colorless oil: R_f = 0.42 (25:75 EtOAc/hexane); ^{1}H NMR ($CDCl_3$) δ (cis/trans isomers) 7.78−7.29 (m, 8H), 4.44 (d, J = 8 Hz, 2H), 4.29 (s, 1H), 4.20 (s, 1H), 4.28−4.24 (m, 1H), 4.20 (s, 1H), 4.07 (s, 1H), 4.04 (s, 1H), 2.91 (q, J = 7.5 Hz, 1H), 2.90 (q, J = 7.5 Hz, 1H), 2.90 (m, 2H), 1.47 (s, 3H), 1.26 (t, J = 7.5 Hz, 1.5H), 1.25 (t, J = 7.5 Hz, 1.5H); ^{13}C NMR δ (cis/trans isomers) 198.0, 197.8, 168.4, 168.3, 156.2, 156.0, 143.9, 141.4, 129.0, 127.3, 125.2, 120.1, 82.4, 68.6, 57.6, 57.3, 50.5, 50.3, 47.2, 28.2, 23.2; ESIMS calcd for $C_{25}H_{29}NO_5S$ 455.57, found 456 (M + H)$^+$. Anal. Calcd for $C_{25}H_{29}NO_5S$: C, 65.91; H, 6.42; N, 3.07. Found: C, 66.20; H, 6.45; N, 3.13.

***N*-(Formylmethyl) *N*-Fmoc-Glycine *tert*-Butyl Ester (5).** Triethylsilane (31.9 mL, 200 mmol) was rapidly added to an ice-cold mixture of **4** (18.2 g, 40 mmol) and 10% Pd−C (2.0 g) in acetone (200 mL) and stirred at 10−20 °C for 30 min. The reaction mixture was filtered through a Celite bed, and the cake was washed with acetone (50 mL). The combined filtrates were concentrated in vacuo and purified by flash column chromatography to afford 14.6 g of **5** (93% yield) as a colorless oil: R_f = 0.38 (35:65 EtOAc/hexane); ^{1}H NMR ($CDCl_3$) δ (cis/trans isomers) 9.67 (s, 06H), 9.37 (s, 0.4H), 9.78−9.73 (m, 8H), 4.52 (d, J = 5.5 Hz, 1H), 4.44 (d, J = 7 Hz, 1H), 4.29−4.23 (m, 1H), 4.11 (s, 1H), 4.01 (s, 1H), 4.00 (s, 1H), 3.83 (s, 1H), 1.47 (s, 9H); ^{13}C NMR δ (cis/trans isomers) 198.7, 168.6, 156.3, 156.0, 143.8, 141.4, 128.0, 127.3, 125.2, 124.8, 120.2, 82.6, 68.6, 68.1, 58.4, 57.7, 50.7, 47.2, 28.2; ESIMS calcd for $C_{23}H_{25}NO_5$ 395.45, found 396 (M + H)$^+$.

3-Phenyl-1(*S*)-[[2′-[*N*″-(9-fluorenylmethoxycarbony)-*N*″-(*tert*-butyloxycarbonylmethyl)]amino]ethylamino]-propionamide (6). Sodium triacetoxyborohydride [NaB(OAc)$_3$H] (9.54 g, 45 mmol) was added to a solution of **5** (11.9 g, 30 mmol) and phenylalanylamide hydrochloride (7.0 g, 35

(47) Chorev, M.; Rubini, E.; Gilon, C.; Wormser, U.; Selinger, Z. *J. Med. Chem.* **1983**, *26*, 129−135.

(48) Sennyey, G.; Barcelo, G.; Senet, J. P. *Tetrahedron Lett.* **1986**, *27*, 5375−5376.

mmol) in DMF (100 mL) and stirred at room temperature for 6 h. The reaction mixture was poured into water (300 mL) and extracted with EtOAc (3 × 200 mL). The combined extracts were washed with water (100 mL), dried, and concentrated in vacuo. Purification by flash column chromatography afforded 14.6 g of **6** (90% yield) as a viscous oil. An analytical sample was further purified by semipreparative RP-HPLC on a Vydac C-18 column, λ = 220 nm, employing a linear gradient of 0−70% (v/v) B in A over 100 min and then lyophilized: mp 60−62 °C; R_f = 0.36 (80:19:1 EtOAc/hexane/TEA); $[\alpha]_D^{20}$ = −20.3° (*c* 0.76, MeOH); ^{1}H NMR ($CDCl_3$) δ (cis/trans isomers) 7.74−7.15 (m, 13H), 6.00 (m, 1H), 4.34 (d, *J* = 7.0 Hz, 1H), 4.18 (m, 1H), 3.73 (d, *J* = 2.5 Hz, 1H), 3.47 (m, 1H), 3.31 (dd, *J* = 9.0, 5.0 Hz, 1H), 3.24−3.15 (m, 3H), 2.77−2.62 (m, 2H), 1.44 (s, 9H); ^{13}C NMR δ (cis/trans isomers) 177.1, 176.8, 168.9, 156.3, 143.9, 141.3, 137.6, 129.1, 128.8, 127.8, 127.2, 126.9, 125.1, 124.8, 120.0, 82.2, 82.0, 68.0, 67.4, 64.3, 64.1, 50.5, 50.1, 49.2, 48.7, 47.3, 47.0, 46.8, 39.4, 39.2, 28.1; ESIMS calcd for $C_{32}H_{37}N_3O_5$ 543.65, found 544 (M + H)$^+$. Anal. Calcd for $C_{32}H_{37}N_3O_5 \cdot {}^1/_3$TFA: C, 67.39; H, 6.47; N, 7.22. Found: C, 67.02; H, 6.68; N, 7.09.

***N*-(*tert*-Butyloxycarbonylmethylcarbonyl) α-(9-Fluorenylmethyl), *β*-Cyclohexyl L-Aspartate (7).** DCC (4.5 g, 22 mmol) was added to a stirred, ice-cold solution of l-α-(9-fluorenylmethyl)-*β*-cyclohexyl-aspartate hydrochloride [H-Asp(OcHex)-OFm][38] (4.3 g, 20 mmol), diisopropylethylamine (DIPEA) (3.5 mL, 20 mmol), and mono-*tert*-butylmalonate (3.2 g, 20 mmol) in DCM (50 mL). After stirring for 30 min at room temperature, the reaction mixture was filtered, and the filtrate was concentrated in vacuo. The residue obtained was purified by flash column chromatography to afford 9.8 g of **7** (92% yield) as a viscous oil: R_f = 0.44 (25:75 EtOAc/hexsane); ^{1}H NMR ($CDCl_3$) δ 7.77−7.25 (m, 8H), 4.80−4.65 (m, 4H), 4.41 (m, 2H), 4.21 (t, *J* = 7 Hz, 1H), 3.04−3.02 (m, 1H), 2.81−2.78 (m, 1H), 1.20−1.79 (m, 28H); ^{13}C NMR δ 171.6, 171.3, 170.6, 167.3, 155.6, 143.8, 141.3, 128.1, 127.4, 125.3, 120.1, 81.4, 73.8, 68.2, 66.4, 50.1, 46.9, 31.6, 28.2, 25.4, 23.9; ESIMS calcd for $C_{31}H_{37}NO_7$ 535.63, found 536 (M + H)$^+$.

***N*-(Carboxylmethylcarbonyl) α-(9-Fluorenylmethyl), *β*-Cyclohexyl l-Aspartate (8).** Compound **7** (8.0 g, 15 mmol) was dissolved in Et_2O (200 mL) and then saturated with HCl (g). The mixture was stored at room temperature overnight, concentrated in vacuo, and vacuum-dried to afford 7.1 g of **8** (100% yield) as a light yellow semisolid. The product became a glasslike solid after storage in the refrigerator for several days. This crude product was used in the subsequent reaction without further purification: R_f = 0.39 (35:65 EtOAc/hexane); ^{1}H NMR ($CDCl_3$) δ 7.77−7.25 (m, 8H), 4.79−4.65 (m, 2H), 4.37 (m, 2H), 4.25−4.22 (m, 1H), 3.04−3.02 (m, 1H), 2.81−2.78 (m, 1H), 1.20−1.79 (m, 19H); ^{13}C NMR δ 171.6, 170.2, 170.6, 167.3, 155.6, 143.8, 141.5, 128.1, 127.4, 125.3, 120.1, 73.8, 67.2, 63.4, 51.1, 45.6, 31.6, 25.4, 23.9; ESIMS calcd for $C_{27}H_{29}NO_7$ 479.52, found 480 (M + H)$^+$.

1-(9-Fluorenylmethyl), 4-Cyclohexyl 2(*S*)-{*N*-[3′-[*N*′-[2″-[[*N*″-(9-Fluorenylmethoxycarbonyl)-*N*″-(*tert*-butyloxycarbonylmethyl)]aminoethyl]-*N*′-[2′-[2′(*S*)-3′-phenylpropionamide]]-1′,3′-dioxopropyl]-amino} Succinnate (9). HATU (1.14 g, 3 mmol) was added to a solution of **6** (1.08 g, 2 mmol), **8** (1.44 g, 3 mmol), and DIPEA (ml, 5 mmol) in DMF (20 mL) and stirred at room temperature for 2 h. This was followed by another portion of HATU (1 mmol), and the mixture was stirred for 2 h. The reaction mixture was concentrated in vacuo, and the residue was dissolved with EtOAc (2 × 50 mL). The solution was washed with $NaHCO_3$ (30 mL) and brine (30 mL), dried, and concentrated in vacuo. Purification of the residue by flash column chromatography afforded 1.85 g of **9** (92% yield) as a viscous oil. An aliquot was dissolved in H_2O-CH_3CN (30:70, v/v) and lyophilized to afford a white powder: mp 69−71 °C; R_f = 0.38 (1:1 EtOAc/hexane); $[\alpha]_D^{20}$ = −18.7° (*c* 0.63, MeOH); ^{1}H and ^{13}C NMR were very complicated due to cis/trans isomers (data not shown); ESIMS calcd for $C_{59}H_{64}N_4O_{11}$ 1105.16, found 1105 (M + H)$^+$. Anal. Calcd for $C_{59}H_{64}N_4O_{11}$: C, 70.50; H, 6.42; N, 5.57. Found: C, 70.06; H, 6.27; N, 5.38.

2(*S*)-[*N*-[[(*N*′-(9-Fluorenylmethoxycarbonyl)-*N*′-(*tert*-butyloxycarbonylmethyl)]aminoethyl]-*N*-[(1′,3′-dioxo-3′-benzyloxy)propyl]]-2-amino-3-phenylpropionamide (11). HATU (380 mg, 10 mmol) was added to a solution of **6** (2.72 g, 5 mmol), monobenzylmalonate (1.94 g, 10 mmol), and DIPEA (2.6 mL, 15 mmol) in DMF (20 mL) and stirred at room temperature for 2 h. The reaction mixture was concentrated in vacuo, and the residue was dissolved in EtOAc (200 mL). The solution was washed with water (100 mL), dried, and concentrated in vacuo. The residue obtained was purified by flash chromatography affording 3.38 g of **11** (94% yield) as a viscous oil. An aliquot was dissolved in H_2O-CH_3CN (30:70, v/v) and lyophilized to afford a white powder: mp 63−65 °C; R_f = 0.42 (1:1 EtOAc/hexane); R_t = 23.84 (20−100% B in A, 30 min); $[\alpha]_D^{20}$= −20.5 (*c* 0.74, MeOH); ^{1}H NMR ($CDCl_3$) δ (cis/trans isomers) 7.77−7.05 (m, 18H), 5.16 (s, 2H), 5.09 (s, 1.1H), 5.05 (s, 0.9H), 4.57−2.86 (m, 12H), 1.46 (s, 9H); ^{13}C NMR δ (cis/trans isomers) 172.4, 168.8, 168.6, 168.3, 156.1, 143.8, 141.4, 135.3, 129.3, 129.0, 128.8, 128.7, 128.5, 128.0, 127.9, 127.4, 127.0, 125.3, 124.7, 120.2, 82.5, 82.1, 68.2, 67.6, 51.3, 48.9, 47.4, 41.2, 38.9, 34.1, 28.2; ESIMS calcd for $C_{42}H_{45}N_3O_8$ 719.82, found 720 (M + H)$^+$. Anal. Calcd for $C_{42}H_{45}N_3O_8$: C, 70.08; H, 6.30; N, 5.84. Found: C, 69.72; H, 6.43; N, 5.76.

2(*S*)-[*N*-[[*N*′-(*tert*-Butyloxycarbonylmethyl)]aminoethyl]-*N*-[(1′,3′-dioxo-3′-benzyloxy)propyl]]-2-amino-3-phenylpropionamide (12). Compound **11** (2.88 g, 4 mmol) was added to 2% DBU in acetonitrile (10 mL) and stirred at room temperature for 30 min. The reaction mixture was concentrated in vacuo and purified by column chromatography affording 2.10 g of **12** (87% yield) as an oil. An aliquot was dissolved in H_2O-CH_3CN (30:70, v/v) and lyophilized to afford a white powder: mp 75−76 °C; R_f = 0.37 (80:19:1 EtOAc/hexane/TEA); R_t = 18.91 min (0−100% B in A, 30 min); $[\alpha]_D^{20}$ = −19.7° (*c* 0.82, MeOH); ^{1}H NMR ($CDCl_3$) δ 7.35−7.15 (m, 10H), 5.66 (m, 1H), 5.15 (m, 2H), 3.56 (s, 2H), 3.42−3.35 (m, 2H), 3.25−3.20 (m, 2H), 3.11−2.95 (m, 2H), 2.83−2.72 (m, 1H), 2.53−2.49 (m, 2H), 1.42 (s, 9H); ^{13}C NMR δ 172.6, 171.0, 167.8, 166.9, 138.5, 135.2, 129.2, 128.9, 128.7, 128.5, 128.4, 126.6, 81.6, 67.5, 51.1, 47.1, 41.7, 33.6, 28.1; ESIMS calcd for $C_{30}H_{44}N_4O_9$ 604.69, found *m*/*z* 605 (M + H)$^+$.

2(*S*)-[*N*-[[(*N*′-(Cyclohexyl 3(*S*)-3-*N*″-Benzyloxycarbonyl-amino-4-oxo-butyrate)]-*N*′-(*tert*-butyloxycarbonylmethyl)]-aminoethyl]-*N*-[(1′,3′-dioxo-3′-benzyloxy)propyl]]-2-amino-3-phenylpropionamide (13). HATU (228 mg, 6 mmol) was added to a solution of **12** (1.81 g, 3 mmol), *β*-cyclohexyl *N*-benzyloxycarbonylaspartate [*N*-Cbz-Asp(OcHex)-OH] (1.89 g, 5 mmol), and DIPEA (1.3 mL, 10 mmol) in DMF (10 mL). The resulting mixture was stirred at room temperature for 4 h and concentrated in vacuo. The residue was extracted with EtOAc (2 × 200 mL), washed with water (100 mL), dried, and concentrated in vacuo. Purification by flash column chromatography afforded 2.15 g of **13** (87% yield) as a viscous oil. An aliquot was dissolved in H_2O-CH_3CN (30:70, v/v) and lyophilized to afford a white powder: R_t = 21.36 (20−100% B in A, 30 min) $[\alpha]_D^{20}$= −21.5° (*c* 0.53, MeOH); ^{1}H and ^{13}C NMR were very complicated due to cis/trans isomers (data not shown); ESIMS calcd for $C_{45}H_{56}N_4O_{11}$ 828.95, found 829 (M + H)$^+$. Anal. Calcd for $C_{45}H_{56}N_4O_{11}$: C, 65.20; H, 6.81; N, 6.76. Found: C, 65.01; H, 6.67; N, 6.42.

2(*S*)-[*N*-[[(*N*′-(Cyclohexyl 3(*S*)-3-Amino-4-oxo-butyrate)]-*N*′-(*tert*-butyloxycarbonylmethyl)]aminoethyl]-*N*-(3′-oxo-propionic acid)-2-amino-3-phenylpropionamide (14). A mixture of **13** (1.66 g, 2 mmol) and 10% Pd−C (160 mg) in 95% methanol (50 mL) was hydrogenated at 40 psi for 2 h, filtered through a Celite bed, concentrated in vacuo, and vacuum-dried to afford 1.17 g of **14** (97% yield) as a white solid. This crude product was used immediately in the subsequent reaction without further purification: R_t = 18.37 min (0−100% B in A, 30 min); ESIMS calcd for $C_{30}H_{44}N_4O_9$ 604.69, found 605 (M + H)$^+$.

1-(*tert*-Butyloxycarbonylmethyl)-3(*S*)-cyclohexyloxycarbonylmethyl-9-[2′(*S*)-3′-phenylpropionamide]-2,5,7-trioxo-1,4,8-triazadecane (10). Compound **14** (907 mg, 1.5 mmol) and DIPEA (0.65 mL, 5 mmol) were dissolved in DMF (50 mL) and added dropwise over 2 h to a solution of HATU (114 mg, 3 mmol) in DMF (100 mL) at room temperature. After 2 h of additional stirring, the reaction mixture was concentrated in vacuo. The residue was extracted with EtOAc (2 × 100 mL) and washed with water (50 mL), and the organic phase was dried and concentrated in vacuo. The residue that was purified by preparative RP-HPLC on a Vydac C-18 column, $\lambda = 220$ nm, employing a linear gradient of 0−70% (v/v) B over 100 min, afforded 490 mg of **10** (56% yield) as a white powder: $R_t = 21.21$ min (0−100 B in A 30 min); $[\alpha]_D^{20} = +6.5°$ (*c* 0.12, MeOH); 1D ^{1}H and ^{13}C NMR were very complicated due to cis/trans isomers (data not shown; ESIMS calcd for $C_{30}H_{42}N_4O_8$ 586.68, found 587 $(M + H)^+$. Anal. Calcd for $C_{30}H_{42}N_4O_8$: C, 61.42; H, 7.22; N, 9.55. Found: C, 61.07; H, 7.47; N, 9.28.

1-(*tert*-Butyloxycarbonylmethyl)-3(*S*)-cyclohexyloxycarbonylmethyl-9-[2′(*S*)-3′-phenyl-propionamide]-2,5,7-trioxo-1,4,8-triazadecane (16). Compound **10** (59 mg, 0.1 mmol) and Me_2S (1 mL) were placed in a Teflon reactor, which was connected to a HF-reaction apparatus. Liquid HF (∼10 mL) was introduced, and the resulting mixture was stirred at 0 °C for 4 h. A residue was obtained after removing the volatile components under vacuum. The residue obtained was dissolved in water (20 mL) and purified by semipreparative RP-HPLC on a Vydac C-18 column, $\lambda = 220$ nm, employing a linear gradient of 0−10% (v/v) B over 100 min. Purification afforded 36 mg of **16** (82% yield) as a white powder: mp 72−74 °C; $R_t = 22.92$ min (0−15% B in A 30 min); detailed ^{1}H and ^{13}C NMR analysis is reported in Tables 1−4; ESIMS calcd for $C_{20}H_{24}N_4O_8$ 448.43, found 449 $(M + H)^+$.

1-(*tert*-Butyloxycarbonylmethyl)-3(*S*)-cyclohexyloxycarbonylmethyl-9-[1′(*R*)-acetamide-2′-phenylethyl]-2,5,7-trioxo-1,4,9-triazadecane (17). Iodobenzene bis(trifluoroacetate) (IBTFA, 107 mg, 0.25 mmol) was added to a solution of **10** (59 mg, 0.1 mmol) in THF−water (2:1, 1.5 mL) at room temperature. Monitoring the reaction by LC-MS revealed that the rearrangement proceeded quantitatively and that the product 1-(*tert*-butyloxycarbonylmethyl)-3(*S*)-cyclohexyloxycarbonylmethyl-9-[1′(*R*)-amino-2′-phenylethyl]-2,5,7-trioxo-1,4,8-triazadecane was stable in solution for hours. $R_t = 18.75$ (0−100% B in A 30 min); ESIMS calcd for $C_{29}H_{42}N_4O_7$ 558.31, found 558.67 $(M + H)^+$.

After the reaction mixture was stirred for 2 h, acetic anhydride (0.94 mL, 1 mmol) was added followed by TEA (1.39 mL, 1 mmol). The reaction mixture was stirred for an additional 2 h and then concentrated in vacuo. Purification of the residue by semipreparative RP-HPLC on a Vydac C-18 column, $\lambda = 220$ nm, employing a linear gradient of 0−70% (v/v) B over 100 min, afforded 50 mg of **17** (84% yield) as a white powder: $R_t = 21.72$ min (0−100% B in A in 30 min); ^{1}H NMR was very complicated due to cis/trans isomers (data not shown); ESIMS calcd for $C_{31}H_{44}N_4O_8$ 600.70, found 601 $(M + H)^+$. Anal. Calcd for $C_{31}H_{44}N_4O_8$: C, 61.98; H, 7.38; N, 9.33. Found: C, 61.43; H, 7.22; N, 9.24.

1,3(*S*)-Bis(carboxymethyl)-9-[1′(*R*)-acetylamide-2′-phenylethyl]-2,5,7-trioxo-1,4,8-triazadecane (18). Compound **17** (30.0 mg, 0.05 mmol) and Me_2S (1 mL) were placed in a Teflon reactor and treated with liquid HF as described for **16**. Purification by semipreparative RP-HPLC on a Vydac C-18 column, $\lambda = 220$ nm, employing a linear gradient of 0−10% (v/v) B over 100 min, afforded 18.5 mg of **18** (86% yield) as a white powder: $R_t = 26.73$ min (0−15% B in A in 30 min); detailed ^{1}H and ^{13}C NMR analysis is shown in Tables 1−4; ESIMS calcd for $C_{21}H_{26}N_4O_8$ 462.45, found 463 $(M + H)^+$.

Nuclear Magnetic Resonance. Peptide solutions were prepared in DMSO (99.9% DMSO-d_6) at a concentration of 5 mM. Proton and carbon spectra were recorded on 400 and 600 MHz spectrometers, respectively, and processed using NMRPipe.[49] ROE cross-peaks were integrated using Felix (Biosym Technologies, Inc.; San Diego, CA). All spectra were referenced to tetramethylsilane.

Proton and carbon assignments were obtained using PE-COSY,[50] TOCSY,[51,52] NOESY,[53,54] and ROESY [55] spectra, recorded in the phase-sensitive mode using the method of States et al.[56] NOESY and ROESY spectra were collected at 298 and 308 K, respectively, with mixing times varying from 150 to 500 ms; the temperature for all other experiments was 298 K. In the ROESY experiments, a spin lock field of 2500 Hz was realized by a series of short pulses as described by Kessler et al.[57] sandwiched between two 90° pulses to compensate for offset effects (compensated ROESY). The typical spectral width was 5200 Hz in both dimensions with 2048 points in f_2 and 600 in f_1, and 32−64 scans were collected at each increment. HMQC[58] spectra were used for the assignment of carbons with directly bonded protons, with 1024 data points collected in the proton dimension and 10 000 Hz and 200 data points for the carbon dimension. Forward linear prediction to 1024 points and zero-filling to 2048 points were applied to the incremented dimension. Gaussian apodization was applied in both the f_2 and f_1 dimensions. The PE-COSY pulse sequence was used for the determination of homonuclear coupling constants. Spectra were acquired at 298 K with 4096 data points in f_2 and 640 incremental data points. HMBC[59] spectra were recorded to determine the magnitude of long-range heteronuclear coupling constants, $^3J_{CH}$, with a spectral width of 20 000 Hz and 2048 data points.

Computational Methods. Metric matrix DG calculations were carried out with a home-written program utilizing random metrization.[60] Experimental distance constraints that were more restrictive than the geometric distance bounds (holonomic restraints) were used to create the final distance matrix.[61] The structures were first embedded in four dimensions and then partially minimized using conjugate gradients followed by distance- and angle-driven dynamics (DADD);[28,62,63] the DADD simulation was carried out at 1000 K for 50 ps with a gradual reduction in the temperature over the next 30 ps. The DADD procedure utilized holonomic and experimental distance constraints plus a chiral penalty function for the generation of the violation "energy" and forces. A distance matrix was calculated from each structure, and the EMBED algorithm[61] was used to calculate coordinates in three dimensions.

Energy minimization and MD simulations were performed using Discover (Consistent Valence Force Field) and Insight II (Molecular Simulations, Inc.). Structures were minimized with the steepest descents and conjugate gradients for 2000 iterations. During the MD simulations, the temperature was gradually raised in 50 K increments from 50 to 300 K with

(49) Delaglio, F.; Grzesiek, S.; Vuister, G. W.; Zhu, G.; Pfeifer, J.; Bax, A. *J. Biomol. NMR* **1995**, *6*, 277−293.
(50) Muller, L. *J. Magn. Reson.* **1987**, *72*, 191−196.
(51) Braunschweiler, L.; Ernst, R. R. *J. Magn. Reson.* **1983**, *53*, 521−528.
(52) Bax, A.; Davis, D. G. *J. Magn. Reson.* **1985**, *65*, 355−360.
(53) Jeener, J.; Meier, B. H.; Bachmann, P.; Ernst, R. R. *J. Chem. Phys.* **1979**, *71*, 4546−4553.
(54) Macura, S.; Huang, Y.; Suter, D.; Ernst, R. R. *J. Magn. Reson.* **1981**, *43*, 259−281.
(55) Bothner-By, A. A.; Stephens, R. L.; Lee, J.; Warren, C. D.; Jeanloz, R. W. *J. Am. Chem. Soc.* **1984**, *106*, 811−813.
(56) States, D. J.; Haberkorn, R. A.; Ruben, D. J. *J. Magn. Reson.* **1982**, *48*, 286−292.
(57) Kessler, H.; Griesinger, C.; Kerssebaum, R.; Wagner, K.; Ernst, R. R. *J. Am. Chem. Soc.* **1987**, *109*, 607−609.
(58) Muller, L. *J. Am. Chem. Soc.* **1979**, *101*, 4481−4484.
(59) Bax, A.; Summers, M. F. *J. Am. Chem. Soc.* **1986**, *108*, 2093−2094.
(60) Havel, T. F. *Prog. Biophys. Mol. Biol.* **1991**, *56*, 43−78.
(61) Crippen, G. M.; Havel, T. F. *Distance Geometry and Molecular Conformation*; John Wiley: New York, 1988.
(62) Kaptein, R.; Boelens, R.; Scheek, R. M.; van Gunsteren, W. F. *Biochemistry* **1988**, *27*, 5389−5395.
(63) Mierke, D. F.; Kessler, H. *Biopolymers* **1993**, *33*, 1003−1017.

500 iterations of dynamics in each increment. The simulations were continued at 300 K for 5000 iterations. Structures were collected every 1000 iterations and energy minimized with the steepest descents and conjugate gradients for 2000 iterations.

Acknowledgment. This work was supported in part by the National Institute of Arthritis and Musculoskeletal Disease, National Institutes of Health (AR42833), Research Foundation through the Cottrell Scholars Program (D.F.M.) and by the Dreyfus Foundation through a Camile and Henry Dreyfus Scholar−Teacher Award (D.F.M.).

Abbreviations Used: COSY, correlation spectroscopy; DADD, distance- and angle-derived dynamics; DBU, 1,8-diazabicyclo[5,4,0]undec-7-ene; DCC, *N*,*N*′-dicyclohexyl carbodiimide; DCM, dichloromethane; DG, distance geometry; DIPEA, *N*,*N*-diisopropylethylamine; DMAP, *N*,*N*-dimethylaminopyridine; DMF, *N*,*N*-dimethylformamide; DMSO, dimethyl sulfoxide; DQF-COSY, double-quantum-filtered COSY; EB, ethylene-bridged; ESI, electron spray ionization; EBRIT-BTM, N_i-to-N_{i+3} ethylene-bridged partially modified retro-inverso tetrapeptide β-turn mimetic; EM, energy minimization; HATU, *O*-(7-azabenzotriazole-1-yl)-1,1,3,3-tetramethyluronium hexafluorophosphate; HMBC, heteronuclear multiple-bond connectivity; HMQC $^{1}H-^{13}C$ heteronuclear multiple-quantum shift correlation; IBTFA, iodobenzene bis(trifluoroacetate); LC−ESIMS, liquid chromatography−electron spray ionization mass spectrometry; MD, molecular dynamics; NMR, nuclear magnetic resonance; NOE, nuclear Overhauser enhancements; NOESY, nuclear Overhauser enhancement spectroscopy; PE-COSY, primitive exclusive COSY; PMRI, partially modified retro-inverso; RMSD, root-mean-square deviation; ROE, two-dimensional rotating frame NOE; ROESY, two-dimensional rotating frame NOE-spectroscopy; RP-HPLC, reversed-phase liquid chromatography; TBA, tetrabutylammonium hydrogensulfate; TEA, triethylamine; TLC, thin-layer chromatography; TMS, tetramethylsilane; TOCSY, total-correlation spectroscopy.

JO011041W